Hamada et al. Int J Concr Struct Mater (2025) 19:15
https://doi.org/10.1186/s40069-024-00741-5

International Journal of Concrete Structures and Materials

RESEARCH

Open Access

Enhancing Concrete Strength and Microstructure with Basalt and Steel Fibers in Acid and Base Environments Incorporating Desert Sand

Hussain M. Hamada[1,2], Farid Abed[1*], Zaid A. Al-Sadoon[3] and Arhum Hassan[4]

Abstract

Concrete is widely used in construction due to its remarkable compressive strength and durability. However, its performance can deteriorate when exposed to harsh environmental conditions, such as acidic or alkaline surroundings. There has been considerable interest in incorporating both basalt and steel fibers (B&SFs) to enhance the resilience of concrete in such challenging settings. This study presents a comprehensive examination of the influence of B&SFs on the strength and microstructure of concrete, utilizing desert sand as a fine aggregate and subjecting it to exposure to acidic and alkaline environments. Employing a systematic experimental approach, this research assesses concrete samples with varying B&SFs proportions. The study encompasses density and compressive strength tests, complemented by microstructural analyses using scanning electron microscopy (SEM) and X-ray diffraction (XRD), to analyze the performance of the concrete under diverse environmental conditions. Initial findings indicate that including B&SFs results in a substantial improvement in concrete strength. The role of basalt fibers (BFs) in enhancing the concrete's resistance to acidic environments by mitigating deleterious effects on microstructural integrity is particularly noteworthy. Notably, when exposed to acidic conditions, concrete mixtures containing 0.5% BFs demonstrated the least strength loss. When B&SFs are synergized, their positive effects are amplified, yielding concrete with exceptional resistance to alkaline environments. Microstructural analysis reveals that incorporating fibers refines and strengthens the interconnected matrix of cementitious products, thereby enhancing cohesion and overall strength. Furthermore, this study underscores that desert sand can be a viable alternative to traditional fine aggregates without compromising concrete resistance if it is appropriately reinforced with fibers. In conclusion, this research sheds light on the promising role of B&SFs in augmenting the strength and microstructure of concrete containing desert sand.

Keywords Basalt and steel fibers, Strength, Microstructure, Desert sand, Acid and base environments

Journal information: ISSN 1976-0485 / eISSN 2234-1315.

*Correspondence:
Farid Abed
fabed@aus.edu
Full list of author information is available at the end of the article

1 Introduction

Concrete, renowned for its exceptional strength and durability, is the preferred choice for various construction projects. Its widespread usage, driven by availability and cost-effectiveness relative to alternative construction materials, has solidified its position in the construction industry (Abu-Jdayil et al., 2019). The burgeoning global population, accompanied by growing infrastructure demands, has catalyzed a surge in construction activities. This surge, in turn, has significantly increased the consumption of concrete, making it an indispensable resource in meeting these evolving construction requirements (Li et al., 2022a). However, substantial concrete production necessitates using copious amounts of cement, both energy-intensive and a significant carbon dioxide (CO2) emission source. In response to the imperative of sustainability and environmental responsibility, the construction industry is progressively shifting towards alternative materials that mimic cement's desirable characteristics. This shift aims to reduce cement dependency and aggregates in concrete production, promoting a cleaner environment and sustainability within the construction sector (Al-Sabaeei et al., 2022). The durability of concrete is a critical factor that determines its suitability for various environmental conditions (Chen et al., 2021) and is defined as its resistance to weathering actions and chemical attacks over extended periods (Khan et al., 2022a). Concrete faces the challenges of sulfate and acid attacks in numerous scenarios, especially in industrial settings. Therefore, incorporating concrete into new structures requires high strength and durability, ensuring longevity in diverse environmental conditions (Amran et al., 2021).

One particularly corrosive agent is sulfuric acid (H_2SO_4), known for its destructive effects on concrete, often leading to structural deterioration (Sharma et al., 2022). Sulfate attacks, driven by chemical reactions and salt crystallization within the concrete matrix, compound this deterioration (Kanaan et al., 2022; Wang et al., 2022). Various types and lengths of fibers are introduced to address the issue of concrete cracking under such circumstances. Hybrid fibers, a combination of basalt and steel fibers (B&SFs), emerge as a promising strategy to enhance concrete durability and fortify it against sulfate and acid attacks, ensuring superior performance in challenging environments (Bankir & Sevim, 2020).

A diverse range of natural and industrial fibers is deployed to reinforce concrete, individually and in hybrid configurations (Li et al., 2020a). Basalt fiber (BF) is notable for its eco-friendliness, inorganic composition, and sustainability. BF emerges as a viable reinforcement material for concrete applications by offering advantages like cost-effectiveness, high tensile strength, non-toxic properties, elevated elastic modulus, excellent thermal stability, and improved strain resistance (Chowdhury et al., 2022; Khandelwal & Rhee, 2020; Saleem et al., 2020). Extensive research has consistently demonstrated the positive impact of BF on concrete durability, particularly in alkaline environments (Li et al., 2022b; Zheng et al., 2021). However, its performance in acid-resistant scenarios is relatively weaker (Khan et al., 2022a). By optimizing BF content, the cement matrix's properties can be significantly improved (Lian et al., 2022).

Recent comprehensive reviews, such as the one by Li et al. (2022c), confirm that including BF enhances concrete's durability, especially in aggressive environments. Furthermore, combining BF with SF in a hybrid configuration has yielded superior performance in concrete structures (Khan et al., 2022a, 2022b). Conversely, adding SF in cement concrete mixtures has been observed to reduce water absorption tendencies (Karimipour & Ghalehnovi, 2021). The recent study by Hamada et al. (Wang et al., 2020) explored the impact of both singular and synergistic applications of steel and basalt fibers on the characteristics of concrete utilizing processed desert sand. This investigation delved into the modifications in concrete performance when reinforced with these fibers, either independently or in conjunction.

The introduction of fly ash (FA) as a cement replacement in hybrid fiber-reinforced concrete (FRC) has demonstrated its potential to enhance the strength and durability of concrete. The spherical shape of FA particles enhances reactivity and packing within the concrete mix, ultimately bolstering its properties (Wang et al., 2020). The synergistic effect of adding both B&SFs to concrete containing FA further enhances strength, durability, and overall performance, crucial factors in resisting the infiltration of chemical substances, such as base and acid ions, into the concrete structure. These infiltrations often manifest as visible cracks, leading to concrete damage (Nazarimofrad et al., 2017).

Elshazli et al. (Afroughsabet et al., 2017) conducted a study to assess the impact of incorporating basalt fibers into concrete on its durability properties. Varied volume fractions of basalt fibers, ranging from 0.15 to 0.50%, were introduced into the concrete mixtures. The findings indicated an enhancement in both the durability and residual strength of the concrete resulting from the addition of basalt fibers. Similarly, Khan et al. (Khan et al., 2022a) explored the effects of basalt and steel fibers on concrete's performance when subjected to long-term exposure to sulfate or acid environments. Their research revealed that the integration of both basalt and steel fibers into the concrete mixtures significantly improved the concrete's durability and strength in aggressive environmental conditions. Furthermore, Koksal et al. (Celestine et al., 2021) investigated the influence of basalt and micro-steel fibers on the durability of mortars. Their study was segmented into three groups containing mixtures with 0.3, 0.6, and 0.9% basalt fibers and 0.25%, 0.5%, and 0.75% steel fibers by volume, respectively. It was observed that a concrete mixture with 0.9% basalt fibers (BF) and 0.75% steel fibers (SF) notably decreased water absorption to a minimal value of 7.8%.

Remarkably, there exists a discernible gap in the extant literature regarding the synergistic impacts of admixtures, specifically fly ash (FA), in conjunction with hybrid fibers (comprising steel and basalt), when employed in concert with desert sand. This research lacuna is particularly evident in studies assessing concrete's compressive strength when subjected to environments characterized by acidic and basic conditions. Such an investigation is crucial for understanding material properties under varying chemical exposures, thereby contributing to the broader field of sustainable construction materials. While research by Nazarimofrad et al. (2017) and Xie et al. (2018) examined the influence of silica fume and SFs on reinforced concrete, their findings primarily centered on load–deflection behavior and compressive toughness. Similarly, investigations into the combined effect of slag and SFs on durability properties showed promising results, emphasizing the positive influence of SFs and slag in concrete mixtures (Afroughsabet et al., 2017).

The primary aim of this study is to explore the impact of integrating basalt and steel fibers (B&SFs) on the durability of concrete when subjected to acidic and basic environments. In pursuit of this objective, ten unique concrete mixtures were formulated, each incorporating varying ratios of B&SFs. Subsequently, these specimens were subjected to both acidic and basic conditions over periods of 28 and 56 days. To quantify the effects of these environmental exposures, the study employed weight loss and compressive strength measurements. A comprehensive microstructural analysis was conducted using scanning electron microscopy (SEM) and X-ray diffraction (XRD) techniques, providing an in-depth understanding of the material changes induced by the environmental conditions.

2 Experimental program

In the present study, the primary raw material utilized was Ordinary Portland Cement (OPC) of Type I, which was selected due to its ready availability in the concrete laboratory and widespread application in general construction. This specific cement type is predominantly employed in fabricating precast elements and various concrete forms that are not intended for use in environments involving direct contact with water or soil. Crushed gravel was used as coarse aggregate with a maximum particle size of 20 mm, desert sand, FA, SF, BF, water, and superplasticizer (SP). The superplasticizer employed is of the polycarboxylic ether type, specifically Master Glenium SKY 504. Tables 1 and 2 present these raw materials' physical properties and chemical composition. The Portland cement was procured from Sharjah Cement Factory in the United Arab Emirates, and the FA was sourced from Elkem Silicon Materials in Norway. The cement adhered to BS EN 197-1 Standards, while the FA complied with ASTM C 1240.

In this investigation, the coarse aggregate was derived from crushed gravel with a maximum particle size of 20 mm, and desert sand was utilized as the fine aggregate. Notably, 95% of the desert sand passed through a 0.3-mm sieve, as illustrated in Fig. 1. Table 3 summarizes the properties of desert sand and coarse aggregates employed in the study.

In this experimental work, the superplasticizer employed is of the polycarboxylic ether type; specifically, Master Glenium SKY 504 as superplasticizer (SP) was used to achieve the desired workability and reduce the water-to-binder ratio in the concrete mixtures. SP is favored when incorporating fibers to facilitate the mixing process. Three different volume fractions of B&SFs were utilized in this study. BFs were introduced at volume fractions of 0.1%, 0.3%, and 0.5%, while crimped steel fiber was used to improve concrete compressive, flexural, and tensile strengths, as also stated by Celestine et al. (2021) and added at volume fractions of 0.5%, 1.0%, and 1.5%. Table 4 shows the properties of basalt and steel fibers used in this study. Additionally, B&SFs were combined into three other concrete mixtures with varying volume fractions, as outlined in Table 5. Owing to the constraints imposed by limited time and resources, the authors could not undertake additional experimental tests. Consequently, this limitation has restricted the scope of deriving a comprehensive understanding of the effects exerted by basalt and steel fibers. Future research could benefit from addressing this gap by conducting more extensive experimental investigations to elucidate these influences in greater detail. A photograph of the B&SFs utilized in this study is displayed in Fig. 2.

Table 1 Physical property of OPC and FA

Physical properties	OPC	FA
Specific gravity	3.15	2.19
Fineness specific surface m^2/kg	374	474.2
Initial setting time (min)	140	
Final setting time (min)	190	
Compressive strength Mortar prism (MPa)	25.7	5.1

Table 2 Chemical composition of binder materials

Binder materials	SiO_2	Al_2O_3	CaO	Fe_2O_3	SO_3	MgO	Na_2O	C_3A	CL	LOI
OPC	19.9	4.81	63.00	3.96	2.80	1.00	0.67	6.05	0.07	3.39
FA	64.5	21.21	9.54	2.8	0.39	0.047	0.21	0.034	0.32	0.92

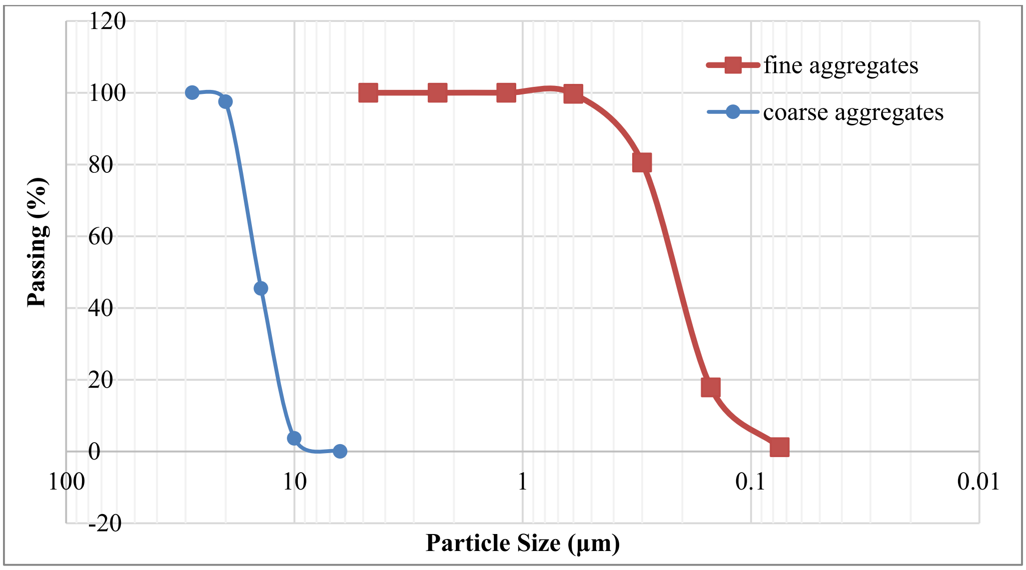

Fig. 1 Distribution curve of coarse and fine aggregates

Table 3 Properties of fine and coarse aggregates

Properties	Fine aggregate (desert sand)	Coarse aggregate
Water absorption (%)	0.8	1.3
Specific gravity (OD)	2.59	2.56
Specific gravity (SSD)	2.61	2.58
Specific gravity (Ap)	2.65	2.63

Table 4 Properties of steel and basalt fibers

Properties	Steel fibers	Basalt fiber
Length-to-diameter ratio	66.6	1000
Diameter (µm)	750	12
Length (mm)	50	12
Tensile strength (MPa)	2850	3000–4000
Elastic modulus (GPa)	201	80–110
Absorption (%)	–	≤ 0.02
Specific gravity	7.9	2.7
Density (g/cm^3)	7.86	2.75

2.1 Mixing and Testing of Concrete

The concrete mixtures were cast into iron molds with precise dimensions of 100 × 100 × 100 mm. Subsequently, these molds were left undisturbed for 24 h at ambient room temperature. Following this initial setting period, the cubic specimens were carefully demolded and placed into a dedicated water tank for curing.

The mixing process was executed with precision. The coarse and fine aggregates were initially introduced into the mixer, which was operated for 3 min. The binder materials, consisting of FA and OPC, were added and mixed for 3 min until a homogeneous mixture was achieved. Half of the required water content was gradually added over 2 min to optimize the consistency of the concrete mix. Subsequently, the SP and the remaining half of the water content were introduced into the mix. For a visual representation of this meticulous mixing and exposure procedure, please refer to Fig. 3.

The concrete samples were divided into two groups to facilitate the study's objectives. One group was placed in a small tank containing an acid solution (H_2SO_4), while the other group was immersed in a separate tank containing a base solution (NaOH). Both groups were subjected to these environmental conditions for 28 and

Table 5 Mix design of B&SFs-reinforced concrete (kg/m^3)

No.	Mix mode	Cement	FA	Fine agg	Coarse agg	Fiber by weight	Water	SP %
CM1	Control	400	100	750	1000	0	200	1
CM2	BF0.1	400	100	750	1000	1.325	200	1
CM3	BF0.3	400	100	750	1000	2.65	200	1
CM4	BF0.5	400	100	750	1000	3.975	200	1
CM5	SF0.5	400	100	750	1000	39.25	200	1
CM6	SF1.0	400	100	750	1000	78.5	200	1
CM7	SF1.5	400	100	750	1000	117.75	200	1
CM8	BF0.1 + SF0.5	400	100	750	1000	1.325 + 39.25	200	1
CM9	BF0.3 + SF1.0	400	100	750	1000	2.65 + 78.5	200	1
CM10	BF0.5 + SF1.5	400	100	750	1000	3.97 + 117.75	200	1

(a) (b)

Fig. 2 Steel and basalt fibers (B&SFs) used in the study: **a** SF and **b** BF

56 days, enabling a comprehensive evaluation of their performance over time.

Table 5 presents a comprehensive breakdown of the concrete mix compositions utilized, encompassing ten distinct mixtures. B&SFs were introduced at varying volume fractions to enhance the experimental investigation's versatility. Three different volume fractions were incorporated into the concrete matrix for each fiber type. The resulting concrete specimens were formed using steel molds to ensure precision and consistency in shape and size. Subsequently, these specimens were subjected to compaction on a vibration table for a duration of 30 s, achieving optimal compaction and uniformity throughout the sample.

2.2 Density and Compressive Strength Tests

The concrete sample density was determined at three distinct curing periods: 1, 28, and 56 days, following the standards outlined in ASTM C138 (Astm, 2013). Additionally, the workability of the concrete was assessed using the slump test, as specified by ASTM C143/143M-15a (Astm, 2015). Compressive strength tests were executed following the guidelines presented in ASTM C39/C39M-17b (A. I. C. C. o., 2014). Six concrete samples

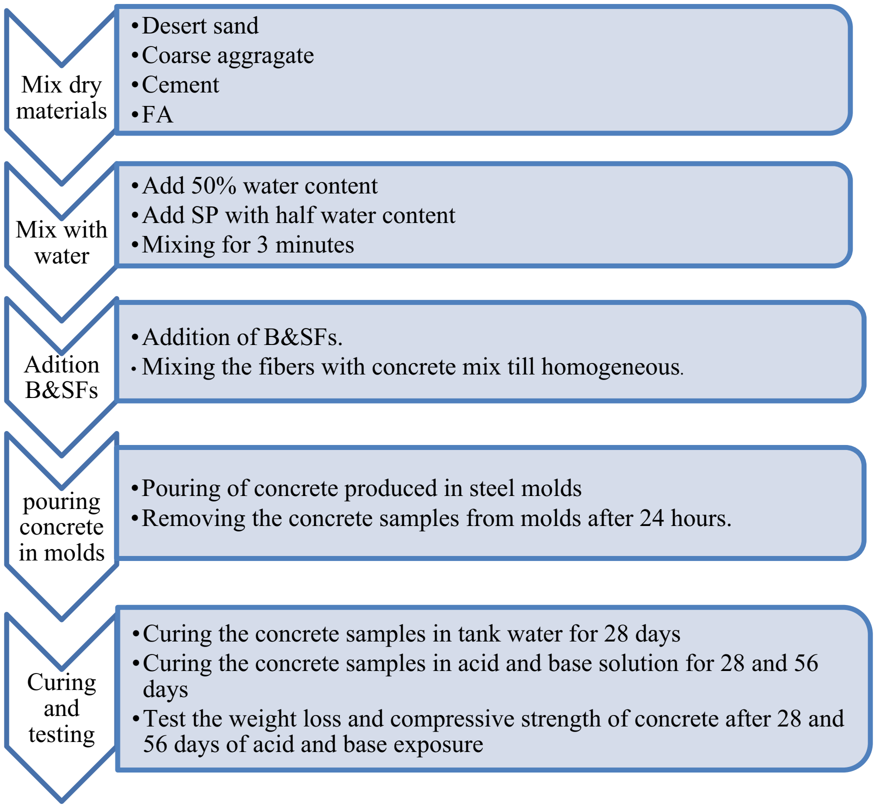

Fig. 3 Mixing process for concrete mix

were prepared for each mix to calculate the compressive strength at two distinct curing ages: 28 and 56 days. Furthermore, an additional set of three concrete samples underwent curing in a water tank for 28 days, facilitating comparative analysis of the results with those obtained from the concrete samples exposed to acidic and alkaline environments.

2.3 Microstructure Tests

Microstructural investigations were conducted employing XRD and SEM methodologies. The concrete samples, in powdered form, were subjected to XRD analysis using a PANalytical X'Pert Pro diffractometer. These samples were derived from concrete mixtures exposed to varying chemical environments, specifically acidic and basic (sulfate) conditions, and were analyzed within a 2θ range of 10^0–40^0. Given that the samples were pulverized for XRD analysis, they were primarily classified into two categories: (a) those containing BFs and (b) those devoid of BFs. This categorization was necessitated by the absence of SFs in the powdered samples; consequently, concrete mixtures CM9 and CM1 were chosen as representative samples for each category. Further, the microstructural characteristics of the hardened concrete were scrutinized using SEM in conjunction with EDS. For this purpose, a representative specimen was extracted from the core of the concrete mixtures (CM1 and CM9), which had been subjected to both acidic and basic environments. The SEM analysis was performed using a Tescan Vega SEM system with an Oxford X-act EDS detector.

3 Results and Discussion

The section presents a comprehensive evaluation of the impact of basalt and steel fibers, as well as their composite forms, on the properties of concrete. This assessment is critical for optimizing concrete mix design and enhancing performance characteristics.

The inclusion of lightweight basalt fibers in concrete is noted to decrease its overall density potentially, contingent on the volume fraction and length of the fibers employed. Conversely, when added to concrete, the denser steel fibers tend to elevate its overall density. This effect is modulated by factors such as the aspect ratio, volume fraction, and the specific geometry of the steel fibers.

When basalt and steel fibers are combined, the resultant effect on concrete's density is intermediate, varying according to the relative proportions of each fiber type. Basalt fibers contribute to the compressive strength of concrete by augmenting its tensile strength and ductility. This enhancement is attributed to the interaction between basalt fibers and the concrete matrix, with a more pronounced effect in tensile and flexural strengths than in compressive strength. On the other hand, steel fibers markedly bolster concrete's compressive strength by improving its toughness and post-cracking behavior. Additionally, they enhance ductility and the capacity for energy absorption.

The synergistic integration of basalt and steel fibers in concrete offers combined tensile strength and toughness benefits. The extent of influence on compressive strength depends on each fiber type's volume fractions and inherent properties. Furthermore, both types of fibers contribute to enhanced crack control and durability of concrete. They play a significant role in mitigating cracking and fortifying the material's resistance to environmental factors. However, the effectiveness of these fibers is influenced by various parameters, including fiber content, aspect ratio, distribution, and the intrinsic characteristics of the matrix material.

In the following subsections, the paper delves into the specific effects of acidic and basic environments on the properties of concrete containing different volume fractions of basalt and steel fibers.

3.1 Effect of Acid Solution on the Concrete

Durable concrete, characterized by its ability to maintain functionality, mechanical strength, and performance under various environmental conditions, is paramount in civil engineering (Amran et al., 2021). This section presents the results and discussion of our investigation into the effects of acid and base solutions on concrete properties. Specifically, the impact of these solutions on the weight, strength, appearance, and microstructure of concrete samples. Initially, all samples were cured in tap water for 28 days before being subjected to acid and base solutions. Subsequently, the weight of the concrete samples was determined in air-curing conditions. Subsequently, the concrete specimens were immersed in a H_2SO_4 solution to simulate acidic conditions. The pH level of the aqueous medium was meticulously adjusted to 2. Throughout this experimental phase, key parameters such as the visual integrity of the concrete, weight loss, and compressive strength were systematically evaluated to ascertain the impact of acidic exposure. Additionally, advanced analytical techniques, including scanning electron microscopy/energy dispersive spectroscopy (SEM/EDS) and XRD, were employed to scrutinize the microstructural alterations in the concrete specimens induced by the acid.

3.2 Effect of Acid on the Appearance of Concrete

The immersion of concrete samples in an H_2SO_4 solution for a 56-day curing period substantially affected their visual characteristics (Fig. 4). The acidic environment induced a brownish appearance on the sample surface, attributed to iron-based oxides. Furthermore, corrosion products were observed on the SFs, leading to a reddish-brown appearance in both fibers and samples.

3.3 Effect of Acid on the Density of Concrete

The density of concrete samples was measured and compared (Fig. 5). BFs, known for their lightweight nature, contributed to a reduction in concrete density when exposed to the acid solution. In contrast, adding SFs led to an increase in concrete density. As the duration of exposure to acid increased, there was a corresponding rise in weight loss in the concrete samples.

The concrete density demonstrated a discernible decline as the BF content increased, as depicted in Fig. 5, specifically, in concrete mixtures labeled as CM2, CM3, and CM4, the incorporation of BFs at concentrations of 0.1%, 0.3%, and 0.5% of the binder weight led to a reduction in concrete density by 1.83%, 2.8%, and 0.55% after one day, respectively. This reduction in density is attributable to the lower specific gravity of BF compared to SF. Conversely, the concrete samples designated as CM10, which contained a hybrid of B&SFs, exhibited superior density relative to the control concrete. The density of CM10 was valued at 2335 kg/m^3, which is higher than the comparable value of the control concrete mix (2322 kg/m^3). This increase is attributed to the addition of steel and basalt fibers to the concrete mixture. A discernible weight loss across all concrete mixtures was observed, suggesting a chemical interaction between the acid solution and the concrete

Fig. 4 Concrete mixture appearance after exposure to an acidic environment before testing

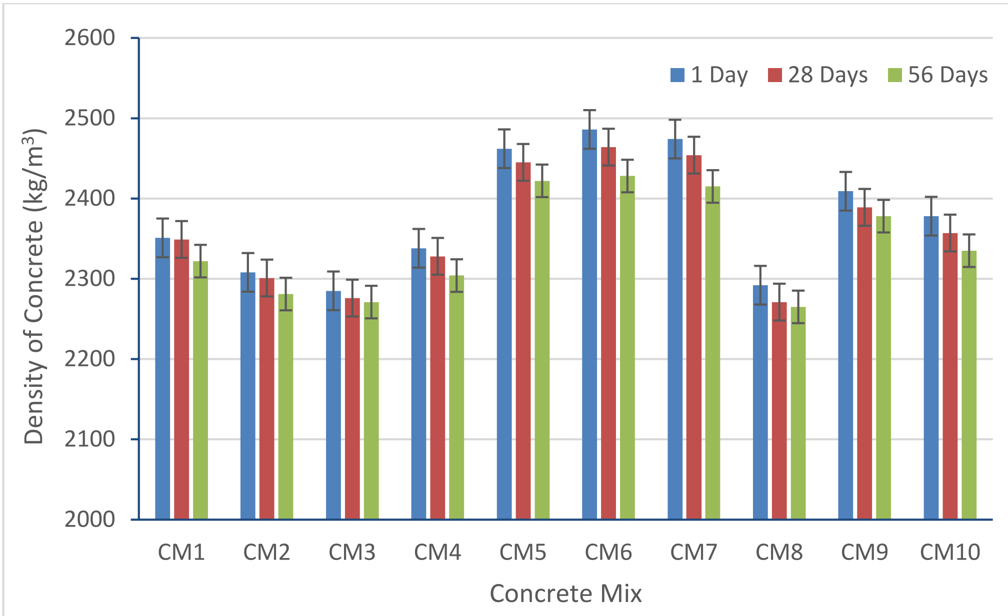

Fig. 5 Effect of acid solution on the density of concrete samples

constituents. This interaction facilitated the absorption of the acid solution into the concrete samples, culminating in a weight loss. These findings are consistent with the results of Khan et al. (Khan et al., 2022a), who employed B&SFs to augment the concrete's resistance to acidic and basic solutions. They reported a marked reduction in the weight of the concrete samples, attributing this to the degradation of concrete in acidic conditions.

Notably, the density of all concrete samples decreased following immersion in H_2SO_4 for periods of 28 and 56 days. The concrete exhibited degradation in the H_2SO_4 solution, leading to weight loss across all mixtures except those containing BF. In samples such as CM2, CM3, and CM4, the weight loss ranged between 0.61 and 1.4%. In contrast, samples devoid of BFs experienced a weight loss between 1.6 and 2.4%. This data substantiates that BF offers enhanced performance in terms of resistance to acidic solutions, as evidenced by the minimal weight loss compared to SF and control samples. The observed reduction in density for the CM8 samples, which incorporated 0.1% BF and 0.5% SF, could potentially be attributed to variations in the compaction parameters within the concrete laboratory. Specifically, the discrepancies in the compaction rate and the duration of compaction might have significantly influenced the resulting material density. This hypothesis underscores the critical impact of standardized laboratory practices on the reproducibility of concrete material characteristics.

3.4 Effect of Acid on the Compressive Strength

The experimental setup employed concrete cubes with dimensions of 100 mm for depth, length, and width. Figure 6 delineates the compressive strength outcomes for all concrete samples subjected to the H_2SO_4 solution exposure over 28 and 56 days. For baseline comparison, control samples were initially cured in tap water for 28 days, and their compressive strength was assessed on Day 1.

The observed decrease in compressive strength across all concrete mixtures with advancing curing age can be primarily attributed to the deleterious interaction between the acid solution (H_2SO_4) and hydration products and the concrete's hydration products. This interaction undermines the structural integrity of the concrete. Acidic environments facilitate the dissolution of both hydrated and un-hydrated cementitious compounds, contributing to a deterioration in compressive strength. This phenomenon aligns with the findings of Khan et al. (Kocan & Hicsonmez, 2019), who reported significant reductions in both the compressive strength and mass of concrete specimens subjected to prolonged exposure to a sulfuric acid solution, extending up to 365 days.

The data presented in Fig. 6 reveal that concrete mixtures with varying volume fractions of B&SFs demonstrated distinct rates of compressive strength degradation when exposed to the acidic medium for 28 and 56 days. This decrement in strength is attributable to the corrosive impact of the acid over the curing duration. Multiple variables, including the composition of B&SFs, the acidic

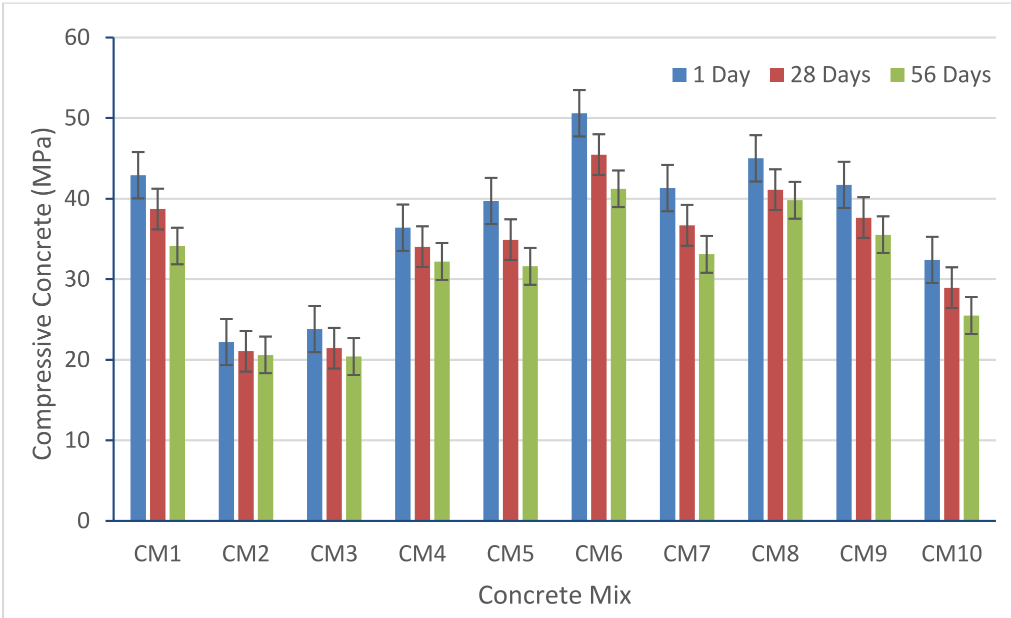

Fig. 6 Effect of acid solution on the compressive strength of concrete

medium, and the curing time, collectively contribute to the observed variations in compressive strength reduction. Notably, the data suggest an inverse relationship between curing age and compressive strength, indicating compromised durability for samples subjected to prolonged acidic exposure.

The high concentration of H_2SO_4 adversely affects the concrete's microstructure, leading to the dissolution of calcium silicate hydrate (C–S–H) gels. This phenomenon weakens the interfacial bonding between the cement matrix and aggregates. The dissolution of C–S–H gels and the subsequent formation of ettringite are identified as primary factors responsible for strength degradation, corroborating the findings of Patel et al. (Attah et al., 2018; Khan et al., 2022a). Incorporating BFs mitigates the strength loss in concrete samples exposed to the acidic environment compared to fiber-free samples (CM1). Concrete mixtures containing solely BFs demonstrated reduced vulnerability to acidic corrosion, consistent with extant literature (Attah et al., 2018; Khan et al., 2022a). Specifically, samples with 0.1%, 0.3%, and 0.5% BF concentrations (CM2, CM3, and CM4) exhibited compressive strength reductions of 7.2%, 14.2%, and 11.5%, respectively, when immersed in H_2SO_4 for 56 days. Conversely, samples containing 0.5%, 1%, and 1.5% SFs registered compressive strength losses of 20.4%, 18.5%, and 19.8%, respectively. These observations align closely with the results reported by Khan et al. (Khan et al., 2022a), who also noted a decrease in compressive strength for concrete samples exposed to acidic conditions compared to those cured in neutral water. The experimental findings reveal that the concrete mixture designated as CM6, which incorporates 1% steel fiber (SF) by volume, exhibited superior compressive strength relative to other tested concrete mixtures. This notable increase in strength can be primarily attributed to including SF at an optimal concentration within the mixture. Supporting this observation, the study conducted by Abbass et al. (Lipatov et al., 2021) corroborates that integrating steel fiber into concrete mixtures contributes to a marginal yet significant enhancement in their compressive strength capabilities. This finding underscores the potential of steel fiber as a reinforcing agent in concrete, optimizing its structural properties.

3.5 Effect of (Sulfate) Base on the Concrete Properties

3.5.1 Effect of Base (Sulfate) on the Appearance of Concrete

The concrete specimens immersed in base solution, specifically sodium hydroxide (NaOH), exhibited a whitish surface, as depicted in Fig. 7. This discoloration can be attributed to the chemical interaction between NaOH and calcium-containing compounds such as gypsum ($CaSO_4.2H_2O$) (Ghorab & Fetouh, 1985) and bassanite ($CaSO_4.0.5H_2O$) (Kocan & Hicsonmez, 2019). This reaction culminates in calcium hydroxide $Ca(OH)_2$ formation, which subsequently leaches onto the surface, imparting a whitish hue. SEM/EDS analyses corroborate this observation.

Fig. 7 Concrete mixture appearance after exposure to the basic environment before testing

3.6 Effect of Base on the Density of Concrete

As illustrated in Fig. 8, the density of concrete specimens exposed to a base environment was evaluated and compared. The incorporation of B&SFs significantly influenced the density of concrete. SFs exerted a more significant impact on the concrete's weight than BFs. However, BFs demonstrated superior resistance to both alkaline and acidic attacks. Notably, the exposure to sodium hydroxide (NaOH) had a negligible impact on the concrete density, especially when compared to acidic environments.

The chemical reactions within concrete materials are predominantly associated with the interaction between calcium hydroxide Ca(OH)2 and sulfate ions SO42- to yield compounds such as gypsum, ettringite, and other expansive corrosion by-products (Zhao et al., 2012). When sulfate ions infiltrate concrete specimens, they react with the hydration products, forming expansive compounds. This process subsequently induces cracking in the concrete samples. These findings are consistent with a study conducted by Lipatov et al. (2021), which demonstrated a reduction in both the weight and mechanical strength of concrete samples following immersion in 0.5M Na_2CO_3 and 1M NaOH solution.

3.7 Effect of Base on the Compressive Strength

The compressive strength of concrete specimens subjected to an alkaline medium, such as NaOH, was less affected than those exposed to acidic conditions. Figure 9 presents the compressive strength values for concrete cubes exposed to alkaline conditions for 28 and 56 days. These specimens were initially cured in a water tank for 28 days and tested as control samples for one day to establish a baseline for comparison.

Figure 9 shows the impact of B&SFs content on the compressive strength of concrete. Over time, most concrete mixtures exhibited a decline in compressive strength, attributable to the high concentration of the alkaline medium. However, the hybrid fiber mix (M10) displayed a mere 0.99% reduction in compressive strength between 28 and 56 days, the lowest among all

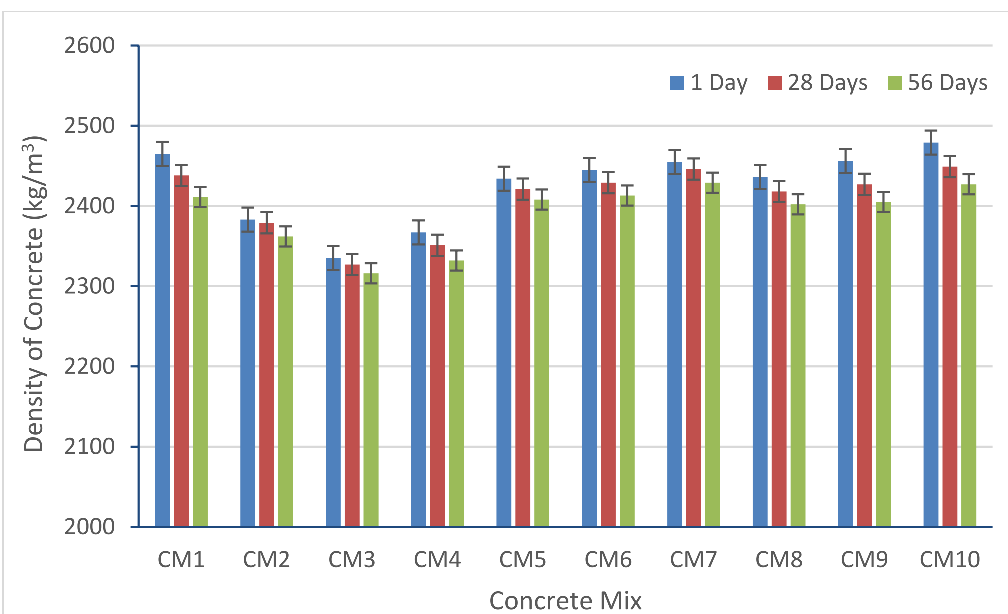

Fig. 8 Effect of base on the density of concrete

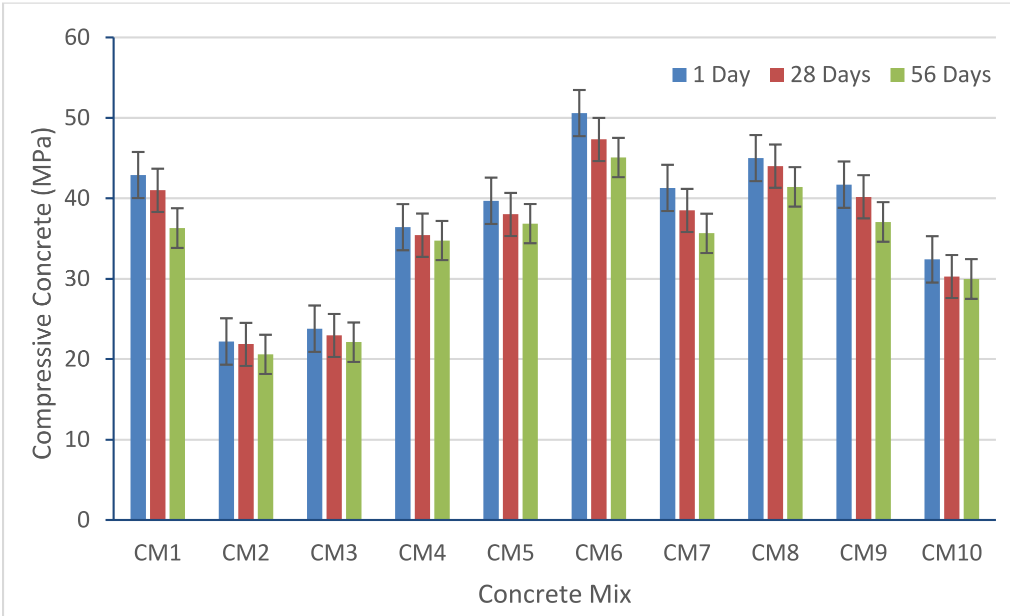

Fig. 9 Effect of base solution on the compressive strength of concrete

tested mixtures. This finding underscores the potential of hybrid fibers in enhancing concrete's resistance to alkaline environments, particularly at high concentrations.

Conversely, concrete containing BFs experienced the least reduction in compressive strength compared to SF-containing and control concretes over 56 days. The percentage reduction in compressive strength for concrete with 0.1%, 0.3%, and 0.5% BF was 7.2%, 7.1%, and 4.5%, respectively. These results agree with prior research conducted by Chindaprasirt et al. (2022). Li et al. (2020b) observed that BF adversely impacts the compressive strength of materials in an alkali-based environment, leading to a significant reduction. Similarly, Khan et al. (2022a) found that the compressive strength of concrete samples varied when exposed to a basic environment, with the extent of reduction contingent upon the composition of B&SFs. Contrarily, Ren et al. (2017) demonstrated that the compressive strength of geopolymer concrete (GPC) diminished upon exposure to various sulfate solutions across different curing periods.

BFs are renowned for their excellent resistance to alkaline substances, including sodium hydroxide. Thus, NaOH's presence is unlikely to significantly impair the performance of concrete containing BFs. It is important to highlight that prolonged exposure to high concentration alkaline solutions may result in the gradual degradation of BF. Elevated concentrations of sodium hydroxide (NaOH) can adversely affect the fiber's mechanical properties over an extended period. Moreover, if the concrete mixture is not meticulously engineered or includes components susceptible to alkaline conditions, this could compromise the overall structural performance of the concrete.

Adherence to established concrete mix design guidelines and manufacturer-specific recommendations for BF is strongly advised to optimize the performance and longevity of such concrete when exposed to alkaline solutions like NaOH.

3.7.1 Effect of Acid and Base Solutions on the Microstructure of Concrete

X-ray diffractometry (XRD) and scanning electron microscopy (SEM) are instrumental in materials science for elucidating materials' structural and morphological characteristics at the microscale and atomic level. XRD elucidates the crystallographic structure of materials, leveraging the phenomenon of X-ray interaction with crystal lattices to produce diffraction patterns. These patterns facilitate the determination of atomic arrangements within the crystal. Samples for XRD analysis encompass a diverse array, including powders, single crystals, and thin films. The X-ray generation and its interaction with the sample's crystal lattice are central to this technique, leading to patterns formed through constructive and destructive interference.

In contrast, SEM employs a focused electron beam to examine sample surfaces. The interaction between the beam and the sample generates signals that are transformed into detailed, high-resolution, three-dimensional representations of the surface morphology. The sample preparation often involves coating it with a conductive material such as gold, enhancing conductivity, and refining image quality. Thus, while XRD is pivotal for crystallographic studies, SEM provides intricate surface morphology insights. The complementary nature of these techniques is instrumental in acquiring a holistic understanding of material properties.

In concrete sample analysis, XRD and SEM emerge as sophisticated techniques offering unique insights. Their application in the study of concrete reveals detailed information on the crystalline structure of minerals, surpassing conventional methods in certain aspects. XRD is particularly adept at identifying different phases within the concrete, including cementitious phases like Portlandite and ettringite. It is also invaluable in evaluating the crystallinity and amorphous content of samples. On the other hand, SEM offers unparalleled imaging resolution, allowing for the visualization of microstructural elements such as aggregates, pores, and cracks in concrete.

The choice of technique in concrete analysis is contingent upon the specific properties and characteristics under scrutiny. XRD and SEM provide in-depth microstructural information, making them indispensable for a comprehensive understanding of concrete composition and structure across various scales. Integrating these methods with complementary analytical techniques can facilitate a more exhaustive assessment of concrete properties.

3.8 X-ray Diffraction (XRD)

The XRD results depicted in Fig. 10 elucidate the primary constituents of the concrete mixture, which include gypsum ($CaSO_4.2H_2O$), bassanite ($CaSO_4.0.5H_2O$), portlandite ($Ca(OH)_2$), mullite ($Al_6Si_2O_{13}$), limestone ($CaCO_3$), silica/quartz (SiO_2), calcium silicate hydrate (CSH), and dolomite ($CaMg(CO_3)_2$). The peaks corresponding to these constituents are symbolically annotated in the figure legend for ease of identification.

Figure 10 presents the XRD analysis of samples with and without BF. The presence of portlandite is discernible at a 2θ peak position of approximately 18°, as cited in Stutzman et al. (2016). Mullite peaks manifest at 22° (Yaping et al., 2008), while limestone peaks are evident at approximately 24°, 36°, and 39° (Kherbache & Bouzidi, 2019). Both acid- and base-treated samples exhibit the characteristic quartz (SiO_2) peak at a 2θ value of approximately 26.5^0, accompanied by other related peaks at approximately 25.5°, 29°, and 37° (Kherbache & Bouzidi, 2019). The peak at around 28° indicates calcium silicate hydrate (CSH) (Narasimha Reddy & Ahmed Naqash, 2019).

Notably, calcium compounds such as gypsum and bassanite are exclusively present in acid-treated samples. Peaks corresponding to dolomite appear at approximately 32° (Stutzman et al., 2016). Gypsum peaks are observed at about 12° (Kontoleontos et al., 2013) and 34° (Failed, 2014), whereas bassanite peaks are detected at approximately 15°, 29°, and 32° (Ye et al., 2021). In contrast, calcium-containing components are largely absent in samples subjected to sodium hydroxide (NaOH) treatment, as illustrated in Fig. 10b. This absence is attributed to the dissolution of gypsum ($CaSO_4.2H_2O$) (Ghorab & Fetouh, 1985) and bassanite ($CaSO_4.0.5H_2O$) (Kocan & Hicsonmez, 2019) in NaOH, resulting in the formation of Ca(OH)2, as described by Eqs. 1 and 2 (Kocan & Hicsonmez, 2019).

$$CaSO_4.2H_2O + 2NaOH \rightarrow Na_2SO_4 + Ca(OH)_2 + 2H_2O \tag{1}$$

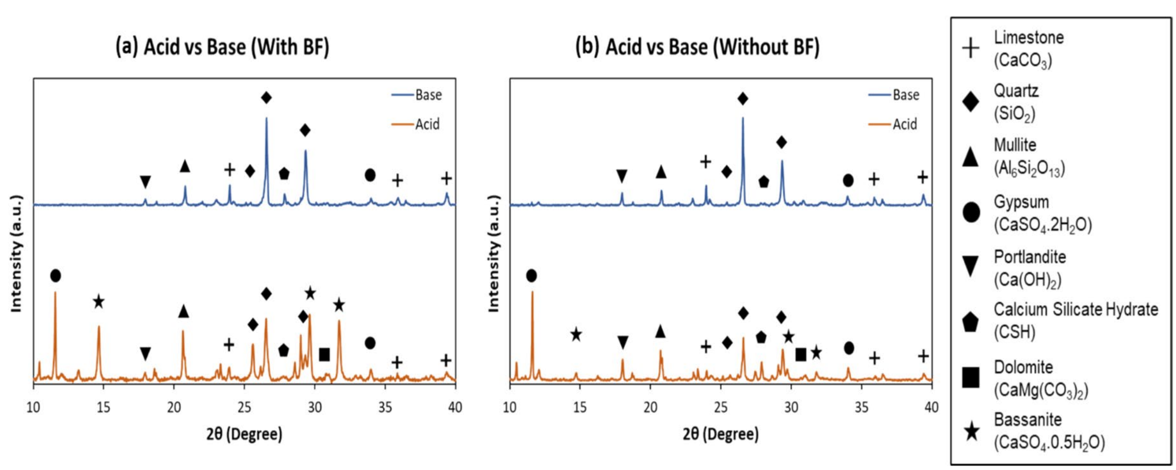

Fig. 10 XRD analysis of samples: a with BF, and b without BF

$$CaSO_4.0.5H_2O + 2NaOH + H_2O \rightarrow Na_2SO_4 + Ca(OH)_2 + 2H_2O \quad (2)$$

The resultant $Ca(OH)_2$ crystals are insoluble and are leached onto the concrete surface. These crystals manifest as small grains with an approximate size of 2µm, as observed through SEM in Fig. 10b. This observation is corroborated by the elevated weight percentage of calcium, as indicated by the EDS of the sample surface exposed to NaOH. The acidic environment had a minimal impact on the samples, thereby preserving all characteristic peaks, as evidenced in Fig. 10a. Furthermore, the detection of BFs via XRD was negligible, owing to their limited size and quantity.

3.9 SEM and EDS

SEM was utilized to investigate the effects of acidic and base treatments on the surface and core morphology of concrete specimens reinforced with fibers. Due to the larger dimensions of SFs, SEM was not employed to assess their environmental impact. BFs exhibited a smooth and lustrous surface in their pristine state, as illustrated in Fig. 11a, with an average diameter measuring approximately 15 µm. However, distinct alterations in surface morphology were observed when the fibers were subjected to varying pH conditions, as evidenced in Fig. 11b and c. Upon exposure to an acidic environment, the BFs displayed notable surface degradation, characterized by visible cracks and delamination, as depicted in Fig. 11b.

Conversely, fibers exposed to an alkaline or base environment demonstrated minimal surface roughness, suggesting a higher resistance to alkaline conditions, as shown in Fig. 11c. Comparative analysis revealed that the fibers subjected to acidic conditions experienced more significant damage than those exposed to a sodium hydroxide (NaOH) environment (Khan et al., 2022a). Additionally, minor hydration products on the fiber surface in both acidic and alkaline conditions indicate satisfactory bonding compatibility between the fibers and the concrete matrix. This observation further suggests favorable fiber–matrix interfacial properties, as Fig. 11b and c corroborated.

The morphological characteristics of the samples displayed notable variations between the core and surface regions when subjected to disparate environmental conditions. Figure 12a, b presents SEM images that elucidate the surface characteristics of the samples following exposure to acidic and basic environments, respectively. As evidenced in Fig. 13a, the concrete surface manifested signs of degradation after interacting with the acidic milieu. This deterioration is further corroborated by an elevated concentration of iron at the surface, as indicated in Fig. 12c. This suggests that iron-containing compounds underwent dissolution in the acidic medium. Given that the dissolved iron was in direct contact with the surface, EDS analysis revealed a heightened presence of iron, as depicted in Fig. 12c.

Conversely, SEM images (Fig. 12b) reveal that samples exposed to a basic environment were characterized by a profusion of minute grains on their surface. Complementary EDS analysis indicated the presence of calcium-containing compounds, inferred from the finely dispersed crystalline structures, as illustrated in Fig. 12d. This phenomenon can be attributed to sodium hydroxide (NaOH) application, which induced decalcification in the concrete samples, thereby liberating calcium ions that migrated to the surface. Consequently, a marked accumulation of calcium products was observed on the concrete surface, in stark contrast to the core region.

As delineated earlier, the core and surface regions exhibited divergent morphological features when exposed to the two distinct environmental conditions. Figure 13a, b provides SEM images of the core region after acidic and basic conditions exposure. Elemental

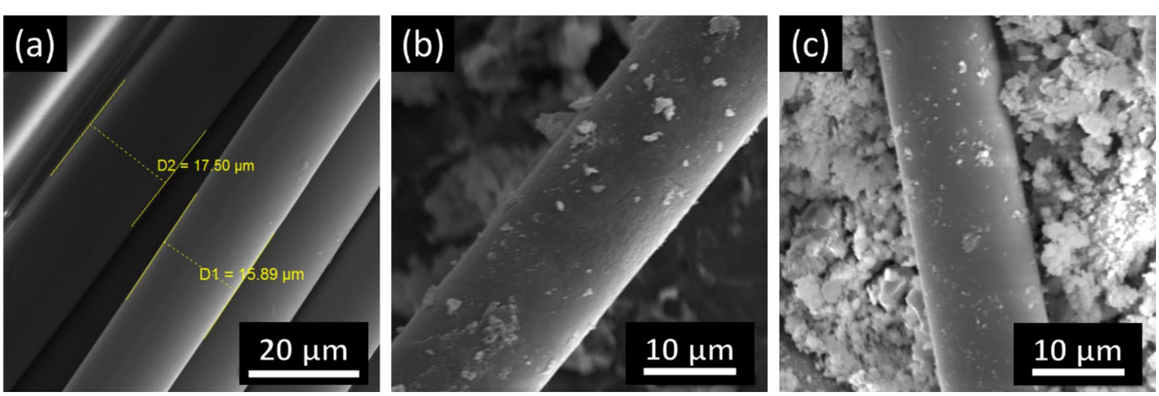

Fig. 11 SEM image of BF in: **a** pristine condition, **b** when exposed to acid, and c when exposed to base

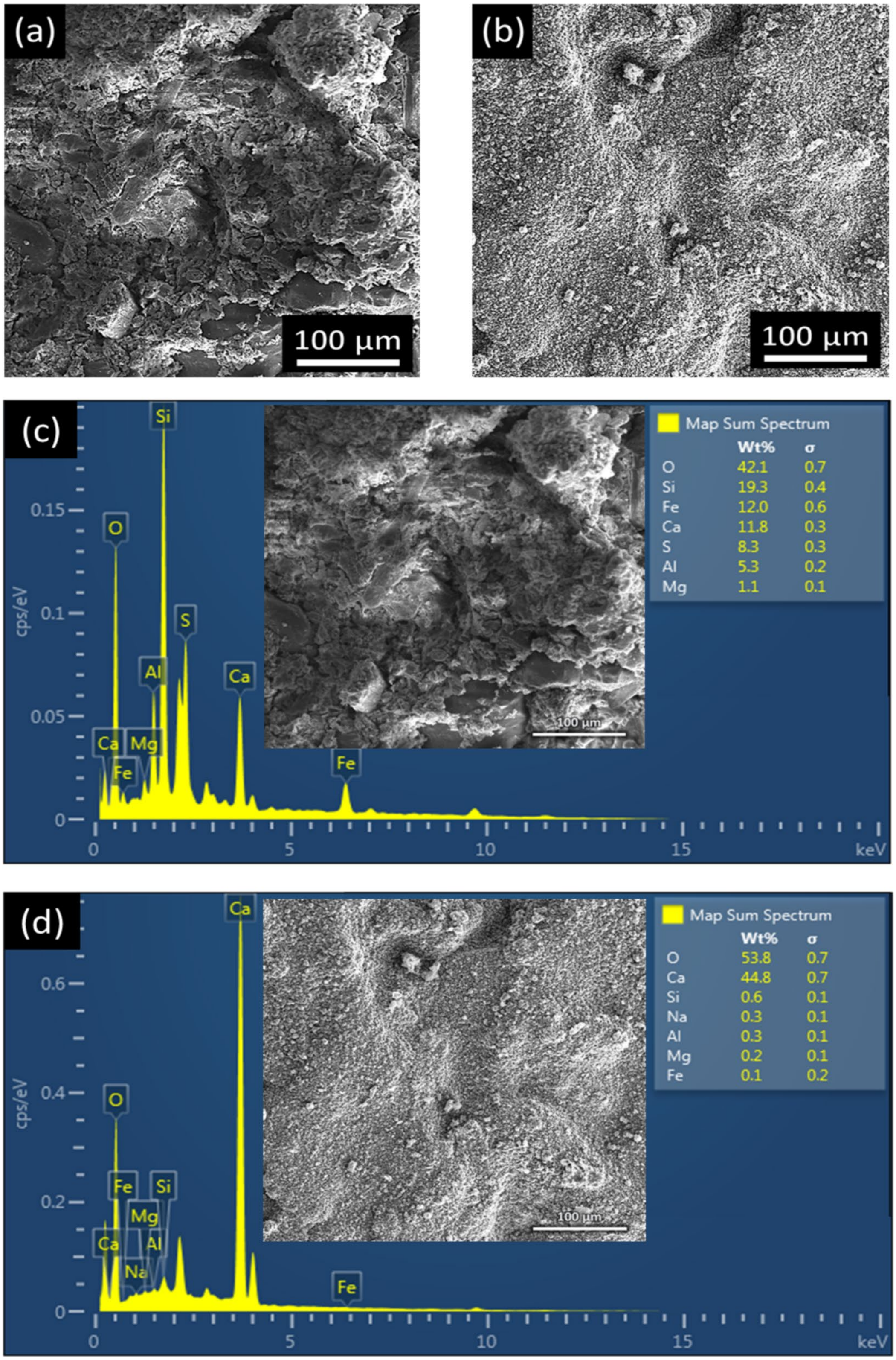

Fig. 12 SEM images and EDS compositional analysis of the concrete surfaces exposed to **a**, **c** acid, and **b**, **d** base

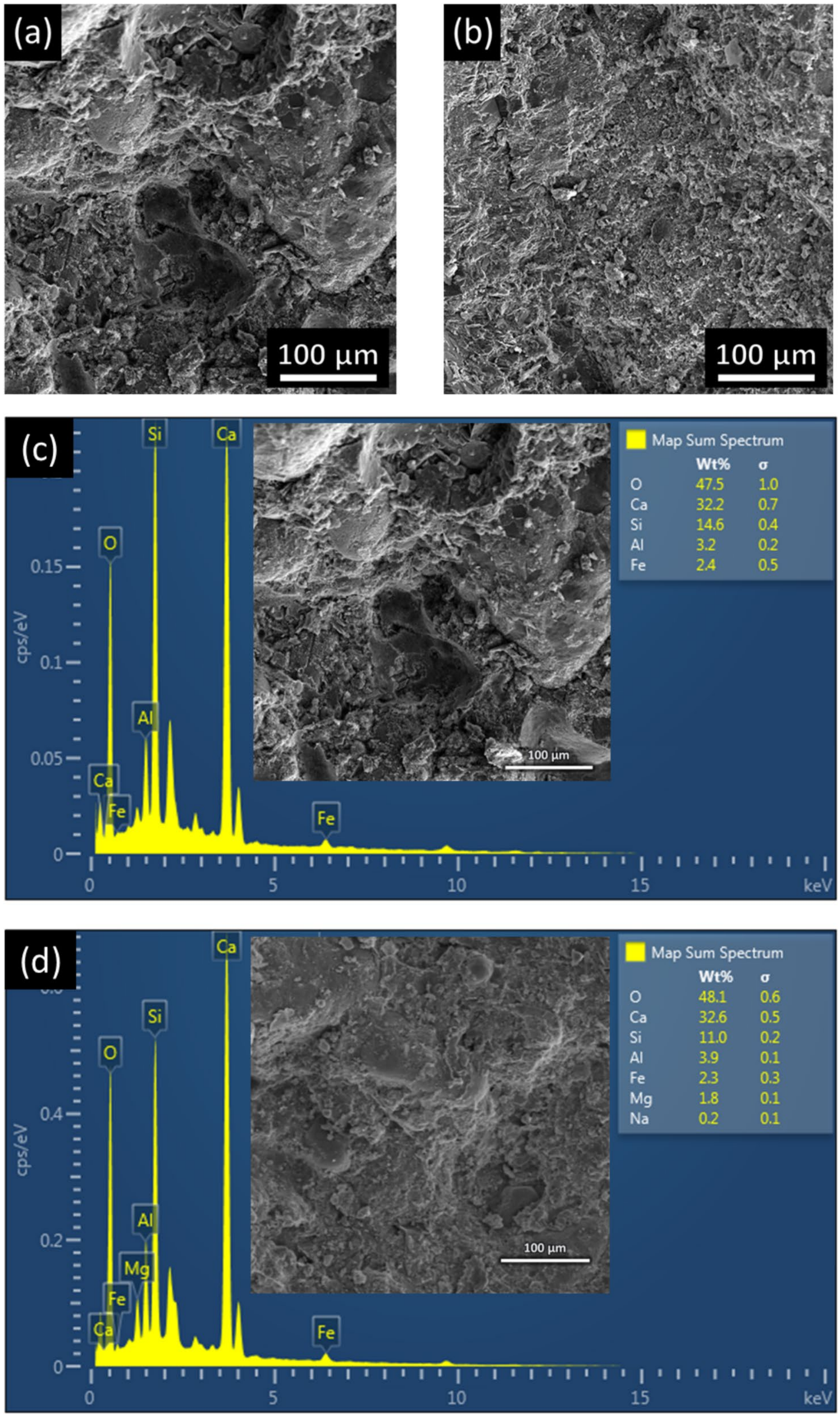

Fig. 13 SEM images and EDS compositional analysis of the concrete core exposed to **a**, **c** acid, and **b**, **d** base

compositions, as presented in Fig. 13c, d, reveal that despite fluctuations in compound composition, as discerned through XRD analysis, the mean elemental composition within the concrete mixture remained relatively invariant. This observation underscores the surface's heightened susceptibility to chemical interactions in acidic and basic milieus, compared to the bulk material. A consistent microstructure was observed in both scenarios, with visible interfacial transition zones.

Additionally, remnants of hydration products were identified within the core, interspersed along the fibers. Notably, samples exposed to acidic conditions demonstrated a diminished mechanical strength, primarily attributable to fiber degradation, as evidenced by microstructural analyses. This degradation exerted a more pronounced impact on the concrete's mechanical integrity relative to basic exposure, as cited in Khan et al., 2022a.

The findings presented in Figs. 12 and 13 are derived from the energy-dispersive X-ray spectroscopy (EDS) analysis of concrete samples. These findings reveal that silica, calcium, and alumina are the predominant elements in the concrete mix, signifying their substantial contribution. The abundance of these elements suggests a more effective pozzolanic reaction due to the inclusion of fly ash (FA) and cement in the mix.

Furthermore, this research introduces the novel use of X-ray diffraction (XRD) and scanning electron microscopy (SEM) techniques to assess the influence of bauxite and silica fumes (B&SFs) on concrete production, especially under various environmental conditions. This methodology significantly shifts from traditional, subjective visual analyses of concrete structures.

4 Conclusion

The primary objective of this study was to investigate the impact of isolated and hybrid B&SFs-reinforced concrete, incorporating desert sand and subjected to both acidic and base environments, on concrete weight and strength. The key findings are summarized as follows:

1. Integrating basalt fibers (BFs) into concrete mixtures exposed to acidic conditions effectively reduced weight loss. The control mix showed a minor reduction from 2351 to 2322 kg/m^3, whereas mixes with BFs (CM4, CM7, CM10) demonstrated more significant decreases, indicating the potential of BFs in enhancing concrete durability in acidic environments.
2. Incorporating varying volume fractions of basalt fibers (BFs) was critical in mitigating the reduction in mechanical strength of concrete subjected to acidic environments. This was evidenced by the superior performance of the BF-enhanced concrete mixes compared to their counterparts. Notably, concrete samples containing 0.5% basalt fiber decreased compressive strength from 36.4 to 32.2 MPa after 56 days of exposure to the acidic solution.
3. While BFs generally reduced weight loss in samples exposed to alkaline conditions, it is noteworthy that the concrete sample designated as CM4, which had high BF content, experienced an increased weight loss.
4. Among the various mixtures investigated, the concrete sample with hybrid fibers (CM10) demonstrated the most minimal reduction in compressive strength when subjected to alkaline conditions over 28 to 56 days.
5. Advanced microstructural analyses employing XRD and SEM revealed that acidic conditions led to the dissolution of iron-based compounds, whereas alkaline conditions resulted in the dissolution of calcium-based compounds.
6. Remarkably, BFs maintained robust fiber–matrix interfacial properties in both acidic and alkaline environments despite suffering more extensive damage from acidic conditions.

This research underscores the imperative of expanding investigations into alternative natural fibers to achieve an equilibrium between cost-effectiveness and environmental sustainability, particularly under adverse conditions. Future studies should adopt a comprehensive approach to elucidate concrete performance, assessing additional vital characteristics such as flexural strength, tensile strength, water absorption capacity, chloride ion penetration, and resistance to freeze–thaw cycles. Moreover, subsequent research endeavors are recommended to explore the augmentation of concrete strength and microstructure by applying varying fraction volumes in diverse acidic and basic environments. Furthermore, there exists a significant opportunity to investigate the synergistic integration of natural fibers with B&SFs positing a potentially optimal strategy for enhancing the eco-efficiency of concrete formulations. These avenues of research are not only pivotal for advancing the field of sustainable construction materials, but also crucial in addressing the broader challenges of environmental sustainability and resource optimization in the construction industry.

Abbreviations

Ap	Appearance dry
BF	Basalt fiber
B&SFs	Basalt and steel fibers
CO_2	Carbon dioxide
EDS	Energy-dispersive spectroscopy
FA	Fly ash
FRC	Fiber-reinforced concrete
H_2SO_4	Sulfuric acid
MPa	Mega Pascal

OPC	Ordinary Portland cement
OD	Oven dry
RC	Reinforced concrete
SF	Steel fiber
SEM	Scanning electron microscopy
SP	Superplasticizer
SSD	Surface saturated dry
XRD	X-ray diffraction

Acknowledgements
The authors want to acknowledge the funding support provided by the American University of Sharjah, Grant number FRG19-L-E23.

Author contributions
Hussein M. Hamada: conceptualization, funding acquisition, and writing a draft paper. Farid Abed: writing, results analysis, and funding. Zaid A. Al-Sadoon: testing, writing, and finalization. Arhum Hassan: testing and writing.

Funding
The work in this paper was supported, in part, by the Open Access Program from the American University of Sharjah. This paper represents the opinions of the authors and does not mean to represent the position or opinions of the American University of Sharjah.

Data availability
Data will be made available on request.

Declarations

Ethics approval and consent to participate
Not applicable.

Consent for publication
Not applicable.

Competing interests
The authors declare that they have no known competing financial interests or personal relationships that could have appeared to influence the work reported in this paper.

Author details
[1]Department of Civil Engineering, College of Engineering, American University of Sharjah, Sharjah, United Arab Emirates. [2]Al-Qalam University College, 36001 Kirkuk, Iraq. [3]Department of Civil and Environmental Engineering, College of Engineering, University of Sharjah, Sharjah, United Arab Emirates. [4]Materials Science and Engineering Program, College of Arts and Sciences, American University of Sharjah, Sharjah, United Arab Emirates.

Received: 23 September 2023 Accepted: 3 November 2024
Published online: 03 March 2025

References

A. I. C. C. o. Concrete and C. Aggregates. (2014). *Standard test method for compressive strength of cylindrical concrete specimens*: ASTM international.

A. C143. (2015). "Standard test method for slump of hydraulic-cement concrete," ed: ASTM International Conshohocken, PA.

Abu-Jdayil, B., Mourad, A.-H., Hittini, W., Hassan, M., & Hameedi, S. (2019). Traditional, state-of-the-art and renewable thermal building insulation materials: An overview. *Construction and Building Materials, 214*, 709–735.

Afroughsabet, V., Biolzi, L., & Ozbakkaloglu, T. (2017). Influence of double hooked-end steel fibers and slag on mechanical and durability properties of high performance recycled aggregate concrete. *Composite Structures, 181*, 273–284.

Al-Sabaeei, A. M., Al-Fakih, A., Noura, S., Yaghoubi, E., Alaloul, W., Al-Mansob, R. A., et al. (2022). Utilization of palm oil and its by-products in bio-asphalt and bio-concrete mixtures: A review. *Construction and Building Materials, 337*, 127552.

Amran, M., Al-Fakih, A., Chu, S., Fediuk, R., Haruna, S., Azevedo, A., et al. (2021). Long-term durability properties of geopolymer concrete: An in-depth review. *Case Studies in Construction Materials, 15*, e00661.

ASTM, A. (2013). "C642-13, Standard Test Method for Density, Absorption, and Voids in Hardened Concrete, ASTM International, West Conshohocken, PA, 2013," ed.

Attah, I., Etim, R., & Ekpo, D. (2018). Behaviour of periwinkle shell ash blended cement concrete in sulphuric acid environment. *Nigerian Journal of Technology, 37*, 315–321.

Bankir, M. B., & Sevim, U. K. (2020). Performance optimization of hybrid fiber concretes against acid and sulfate attack. *Journal of Building Engineering, 32*, 101443.

Celestine, A. K., Prakash, M., Satyanarayanan, K., Surya, T. R., & Parthasarathi, N. (2021). The interpretation of mechanical study of concrete using crimped steel fibres. *Materials Today: Proceedings, 40*, S88–S92.

Chen, K., Wu, D., Xia, L., Cai, Q., & Zhang, Z. (2021). Geopolymer concrete durability subjected to aggressive environments—A review of influence factors and comparison with ordinary Portland cement. *Construction and Building Materials, 279*, 122496.

Chindaprasirt, P., Sriopas, B., Phosri, P., Yoddumrong, P., Anantakarn, K., & Kroehong, W. (2022). Hybrid high calcium fly ash alkali-activated repair material for concrete exposed to sulfate environment. *Journal of Building Engineering, 45*, 103590.

Chowdhury, I. R., Pemberton, R., & Summerscales, J. (2022). Developments and industrial applications of basalt fibre reinforced composite materials. *Journal of Composites Science, 6*, 367.

Ghorab, H. Y., & Fetouh, S. H. A. E. (1985). Factors affecting the solubility of gypsum: II. Effect of sodium hydroxide under various conditions. *Journal of Chemical Technology and Biotechnology Chemical Technology, 35*, 36–40.

Kanaan, D., Soliman, A. M., & Suleiman, A. R. (2022). Zero-cement concrete resistance to external sulfate attack: A critical review and future needs. *Sustainability, 14*, 2078.

Karimipour, A., & Ghalehnovi, M. (2021). Influence of steel fibres on the mechanical and physical performance of self-compacting concrete manufactured with waste materials and fillers. *Construction and Building Materials, 267*, 121806.

Khan, M., Cao, M., Chu, S., & Ali, M. (2022a). Properties of hybrid steel-basalt fiber reinforced concrete exposed to different surrounding conditions. *Construction and Building Materials, 322*, 126340.

Khan, M., Cao, M., Xie, C., & Ali, M. (2022b). Effectiveness of hybrid steel-basalt fiber reinforced concrete under compression. *Case Studies in Construction Materials, 16*, e00941.

Khandelwal, S., & Rhee, K. Y. (2020). Recent advances in basalt-fiber-reinforced composites: Tailoring the fiber-matrix interface. *Composites Part b: Engineering, 192*, 108011.

Kherbache, S., & Bouzidi, N. (2019). Concretes properties made with machining reject (foundry sand).

Kocan, F., & Hicsonmez, U. (2019). Leaching of celestite in sodium hydroxide solutions and kinetic modelling. *Journal of Dispersion Science and Technology, 40*, 43–54.

Kontoleontos, F., Tsakiridis, P., Marinos, A., Katsiotis, N., Kaloidas, V., & Katsioti, M. (2013). Dry-grinded ultrafine cements hydration. physicochemical and microstructural characterization. *Materials Research, 16*, 404–416.

Li, M., Gong, F., & Wu, Z. (2020b). Study on mechanical properties of alkali-resistant basalt fiber reinforced concrete. *Construction and Building Materials, 245*, 118424.

Li, M., Pu, Y., Thomas, V. M., Yoo, C. G., Ozcan, S., Deng, Y., et al. (2020a). Recent advancements of plant-based natural fiber–reinforced composites and their applications. *Composites Part b: Engineering, 200*, 108254.

Li, Y., Zhang, J., He, Y., Huang, G., Li, J., Niu, Z., et al. (2022b). A review on durability of basalt fiber reinforced concrete. *Composites Science and Technology, 225*, 109519.

Li, Z., Zhou, X., Ma, H., & Hou, D. (2022a). *Advanced concrete technology*. John Wiley & Sons.

Lian, H., Sun, X., Yu, Z., Yang, T., Zhang, J., Li, G., et al. (2022). Research on the fracture mechanical performance of basalt fiber nano-CaCO3 concrete based on DIC technology. *Construction and Building Materials, 329*, 127193.

Lipatov, Y. V., Gutnikov, S. I., & Lazoryak, B. I. (2021). Zr-rich basalt continuous fibers with increased alkali resistant properties. *Construction and Building Materials, 288*, 123089.

Narasimha Reddy, P., & Ahmed Naqash, J. (2019). Experimental study on TGA, XRD and SEM analysis of concrete with ultra-fine slag. *International Journal of Engineering, 32*, 679–684.
Nazarimofrad, E., Shaikh, F. U. A., & Nili, M. (2017). Effects of steel fibre and silica fume on impact behaviour of recycled aggregate concrete. *Journal of Sustainable Cement-Based Materials, 6*, 54–68.
Ren, D., Yan, C., Duan, P., Zhang, Z., Li, L., & Yan, Z. (2017). Durability performances of wollastonite, tremolite and basalt fiber-reinforced metakaolin geopolymer composites under sulfate and chloride attack. *Construction and Building Materials, 134*, 56–66.
Saleem, A., Medina, L., Skrifvars, M., & Berglin, L. (2020). Hybrid polymer composites of bio-based bast fibers with glass, carbon and basalt fibers for automotive applications—A review. *Molecules, 25*, 4933.
Sedaghat, A., Ram, M. K., Zayed, A., Kamal, R., & Shanahan, N. (2014). Investigation of physical properties of graphene–cement composite for structural applications. *Open Journal of Composite Materials*. https://doi.org/10.4236/ojcm.2014.41002
Sharma, R., Pei, J., & Jang, J. G. (2022). Resistance of carbonation-cured belite-rich cement mortar to adverse environments: Magnesium sulfate and sulfuric acid exposure. *Cement and Concrete Composites, 134*, 104781.
Stutzman, P. E., Feng, P., & Bullard, J. W. (2016). Phase analysis of Portland cement by combined quantitative X-ray powder diffraction and scanning electron microscopy. *Journal of Research of the National Institute of Standards and Technology, 121*, 47.
Wang, A., Zheng, Y., Zhang, Z., Liu, K., Li, Y., Shi, L., et al. (2020). The durability of alkali-activated materials in comparison with ordinary Portland cements and concretes: A review. *Engineering, 6*, 695–706.
Wang, R., Zhang, Q., & Li, Y. (2022). Deterioration of concrete under the coupling effects of freeze–thaw cycles and other actions: A review. *Construction and Building Materials, 319*, 126045.
Xie, J., Zhang, Z., Lu, Z., & Sun, M. (2018). Coupling effects of silica fume and steel-fiber on the compressive behaviour of recycled aggregate concrete after exposure to elevated temperature. *Construction and Building Materials, 184*, 752–764.
Yaping, Y., Xiaoqiang, Z., Weilan, Q., & Mingwen, W. (2008). Synthesis of pure zeolites from supersaturated silicon and aluminum alkali extracts from fused coal fly ash. *Fuel, 87*, 1880–1886.
Ye, C., Sklute, E. C., & Glotch, T. D. (2021). Orientation averaged visible/near-infrared and mid-infrared optical constants of hydrous Ca-sulfates: Gypsum and Bassanite. *Earth and Space Science, 8*, e2021EA001834.
Zhao, M. L., Wang, S. Q., & Li, A. X. (2012). The study on sulfate resistance of concrete containing admixture mineral. *Applied Mechanics and Materials, 174*, 1265–1268.
Zheng, Y., Zhuo, J., & Zhang, P. (2021). A review on durability of nano-SiO2 and basalt fiber modified recycled aggregate concrete. *Construction and Building Materials, 304*, 124659.

Publisher's Note

Dr. Hussein M. Hamada is a Lecturer in Civil Engineering at Al-Qalam University College, Kirkuk 36001, Iraq. He received his Ph.D. in Civil Engineering from the University Malaysia Pahang, Pahang, Malaysia in 2021. He has published 60 papers in the SCOPUS journals. His primary research in the use of waste materials in the production of sustainable concrete.

Dr. Farid Abed is a Professor of Civil Engineering at the American University of Sharjah (AUS). He earned his PhD degree in 2005 in structures/mechanics from Louisiana State University, USA. His M.Sc. is from the Jordan University of Science and Technology (JUST) in 1997 and his B.Sc. is from University of Technology, Baghdad in 1992. Dr. Abed's research interests include computational solids and structural mechanics, mechanics of concrete and composites, FRP-reinforced and strengthened concrete, and nonlinear finite element. He has secured several national and international grants with more than 5M AED in research funds. He has supervised more than 20 MSc and PhD students and his contributions in his areas of specialization have been published in more than 150 articles in refereed journals and well-known conferences. Dr. Abed is currently a Fellow of the American Society of Civil Engineers (ASCE) and member of the American Society of Mechanical Engineers (ASME). He is also a registered professional engineer (PE) at the state of Louisiana, USA.

Dr. Zaid A. Al-Sadoon is an Associate Professor of Civil Engineering at the University of Sharjah. He received his Ph.D. in Civil Engineering from the University of Ottawa, Canada, in 2016. He is a member of ACI 369 (Seismic Repair and Rehabilitation), ACI 374 (Performance-Based Seismic Design of Concrete Buildings), and ACI 370 (Blast and Impact Load Effects). His primary research interests include seismic risk mitigation and design of earthquake-resistant concrete structures, seismic repair and retrofit of concrete and steel structures, performance-based seismic design, buckling restrained braces, and dynamic time history inelastic analysis. He is the principal and co-investigator on several research grants and has published extensively in refereed journals and conferences on seismic retrofitting, concrete structures, and innovative materials. He Holds three international patents on buckling restrained braces. He is a member of Professional Engineers Ontario (PEO), the Canadian Association for Earthquake Engineering (CAEE), the American Concrete Institute (ACI), the Canadian Society for Civil Engineering (CSCE), and other prestigious organizations.

Arhum Hassan is a PhD student at the Materials Science and Engineering Program at the American University of Sharjah.